# INVESTIGATION OF HEAT FLUX AND EFFUSION/FILM COOLING EFFICIENCY OVER A SHARP CONE SURFACE AT HIGH SUPERSONIC SPEEDS

Pavel V. Chuvakhov Central Aerohydrodynamic Institute (TsAGI), Moscow Institute of Physics and Technology (MIPT)

**Keywords:** film cooling, RANS, turbulence, supersonic separated flows

#### **Abstract**

Results of numerical investigation of both flow structure and surface heat flux over a sharp cone with cooling gas injected out of its surface are presented. Three types of injection are considered, namely: injection through a continuous circular slot on the cone surface in downstream and upstream direction, injection through a porous piece of the surface. Validation with experimental data of TsAGI is conducted. Application of such a heat flux control unit to a simple axisymmetric air inlet with conic central body is studied with an emphasis on total pressure losses. Intensive local cooling effect is found to rise as coolant mass rate increases, with downstream injection having the best efficiency and leading to the least perturbations in outer flow structure. It's found that downstream injection produces the least total pressure losses. However one should find an optimal state between cooling efficiency and total pressure losses for applications.

#### 1 Introduction

Gas moving at high supersonic speeds is heated up when slowed down near a streamed surface. This may result in excessive thermal loads to the surface, which can lead to its being overheated and finally destructed. In order to prevent damage of this type heat protection systems are used. Passive protection (e.g. ablating covers) appears to be simple in use. However it is sometimes of practical importance to preserve original shape of

a surface to provide a room for its repeated use. Active heat protection, e.g. effusion/film cooling (here and after it is simply referred to as film cooling), is an urgent alternative in these cases. This technique of injecting a layer of a cold gas near the surface is implemented via various slot devises and has been used for inner flows for a long time. For example, active heat protection has been applied to practical problems of cooling turbine blades [1], combustor liners [2] and rocket nozzles [3].

Film cooling approach has been investigated earlier both experimentally and numerically for different problem configurations. For instance, experimental studies of tangential slot injection at Mach 6 [4, 5] shows that the film cooling in two-dimensional high speed turbulent flow is significantly more effective then indicated by simple extrapolations of low speed results to high speeds. The same problem configuration is considered in three-dimensional case [6] where coolant is supplied by a tangential step slot at some sweep angle to the outer stream propagation. It is found that cooling effectiveness is not significantly affected by sweeping the slot. [7] presents heat flux results which indicate the effect of divergence on film cooling on a cone at angle of attack. In [8] reduction in drag due to friction is obtained for M = 6 flow by direct measurements in case of coolant injection in downstream direction through both a single and multiple flush slots at small inclination angle to the surface. It is noted as well that tangential injection through a step slot appears to be more effective in friction drag (and consequently heat flux) reduction. In [9] hypersonic flow over a flat plate with blunt leading edge is considered. Layer of cold gas is supplied by a step slot located at the bluntness region. It has been shown that it is possible to protect a region of the stagnation point by tangential injection in upstream direction, with coolant layer traveling along the surface without separation.

The technique of film cooling at supersonic speeds is investigated extensively nowadays. For example, in [10, 11, 12, 13] results of numerical parametric studies of the influence of governing parameters (Reynolds number, Mach number, wall temperature) and injection setup effects (hole spacing, blowing ratio, etc.) on cooling efficiency are presented for laminar boundary layer; [14] deals with turbulent boundary layer; [15, 16, 17] give results of similar experimental investigations for different states of boundary layer.

Unfortunately most of works devoted to film cooling problems consider internal flow prob-There are not enough data for external ones, which has been attractive to scientists for more then sixty years but has not been put in real practice yet. This is explained by both considerable difficulties in realization of film cooling systems and possibility to obtain the sufficient cooling effect by using passive heat protection that is much simpler to apply. In this work different approaches to perform film cooling protection of a sharp cone at high supersonic speeds are investigated. The coolant (air) is supplied via a continuous circular slot in downstream and upstream direction as well as through a porous piece of cone surface. Flow structure and cooling effectiveness are studied. Total pressure losses are evaluated for the case of simple supersonic axisymmetric inlet with conical central body.

#### 2 The Models

Calculations are performed for three different models. The first is designed to perform coolant injection from the cone surface in downstream direction (see fig. 1).

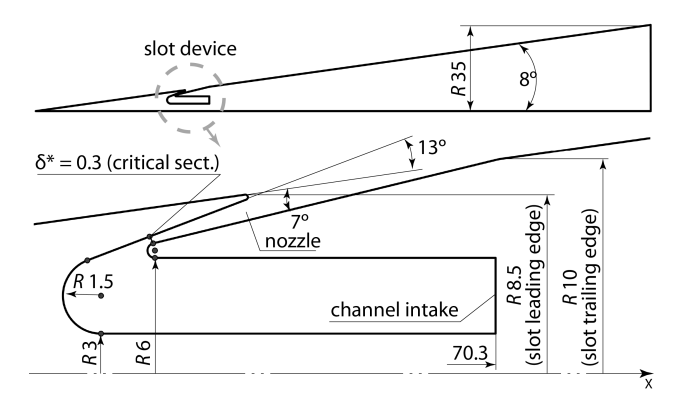


Fig. 1 Model 1, downstream injection

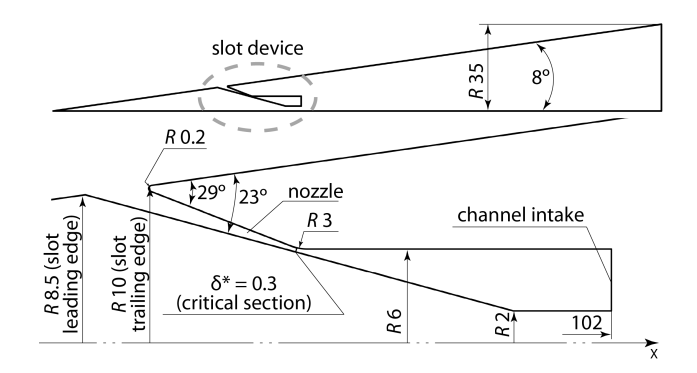


Fig. 2 Model 2, upstream injection

The second model is a solid cone. It is intended for modeling injection process through a porous piece of the surface by imposing a boundary condition of mass rate equally spaced over the piece surface. The third model is dealt with injection in upstream direction (see fig. 2).

For models 1 and 3 the flow inside the slot device is modeled. It begins at channel intake cross section, where the coolant is considered to be at rest. Then it is accelerated by pressure gradient along a channel that finally converges to a critical section. Downstream the critical section is the nozzle coming out from the interior of the model to outer flow.

#### 3 Numerical Problem Formulation

Numerical part of the investigation has been performed on the basis of Ansys Fluent software. A flow of viscous perfect gas with constant Prandtl number is considered in the frame of unsteady RANS equations. Molecular viscosity is calculated according Sutherland's formula. Turbulent

closure  $k-\omega$  transitionSST is used. It makes it possible to model laminar-turbulent transition (LTT) in boundary layer near the slot, which is discussing later. The use of this particular closure is important when coolant is injected in upstream direction. In this case one can expect separation regions to arise upstream the slot position. It is here that one has to realize whether the flow is laminar or turbulent downstream the separation point. This ambiguity can be eliminated by additional experimental investigation.

Density-based implicit coupled solver with second order approximation in space and time is used. Roe method is used to approximate convective part of numerical fluxes. Flow modeling around the models 1, 2, 3 have been performed on structured multiblock grids with total nods count of about 415000, 500000 and 550000, respectively. Computational grid lines are clustered near the solid surface so that a boundary layer close to the slot leading edge turns out to be resolved with about 100 grid lines. A turbulent boundary layer is well-resolved, with about 10 grid lines being inside a laminar sublayer. Noslip conditions (u = 0, v = 0) are imposed onto the boundary corresponding to the cone surface that is considered to be isothermal ( $T_w = 288 \text{ K}$ ). This conforms to the wind tunnel UT-1M experiments. The temperature rise of the model surface is approximately 10 K during an experiment which takes no more than 40 msec. Far field conditions were imposed onto the outer boundary of a calculation region: (1) Here  $T_0$ ,  $p_0$ ,  $M_{\infty}$ , γ are stagnation temperature, total pressure, free stream Mach number, and specific heat ratio consequently. Symbol ∞ relates to free stream values. These parameters result in the unit length Reynolds number  $Re_{\infty,1}3.85 \times 10^7 \, m^{-1}$ . Flow inlet condition is set on the channel intake. Air is considered as cooling gas. Its stagnation temperature is  $T_{j,0} = T_w = 288$  K and total pressure varies among  $p_{i,0} = 1, 2, 4, 8$  bar, in accordance with the experiments. Hereafter, a notation subscripted by *j* relates to coolant.

Results of calculations on a coarse grid are interpolated onto the fine grids and then used as initial estimations for the numerical problem involved. All calculations are carried out to obtain

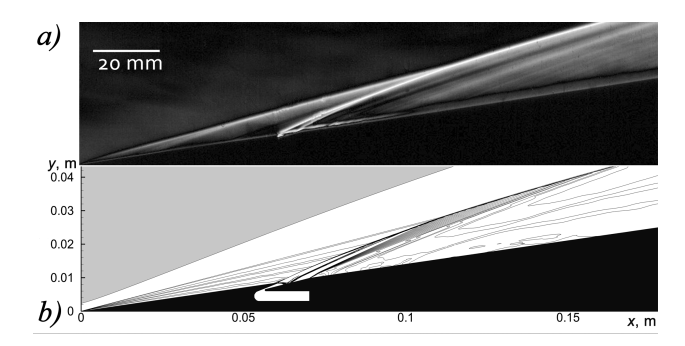


**Fig. 3**  $p_{j,0}$ = 8 bar. a) experiment [18]; b) pressure field, present calculation.

solutions that are stationary in time using timedependent solver.

#### 4 Results

To apply active thermal protection methods requires estimation of coolant mass flow rate  $G_j$ . It is clear that  $G_j$  varies with  $p_{j,0}$ . The dependencies of  $G_j$  on  $p_{j,0}$  are obtained from calculations and presented in table 1 in the dimensionless form. There the coolant  $\ddot{\text{nh}}$ Cow rate is normalized by the air  $\ddot{\text{nh}}$ Cow rate in the free stream,  $G_{\infty} = \rho_{\infty} V_{\infty} \pi R^2$ , through the section that is a circle of R = 35 mm. Coolant mass rate is calculated via the following formula:

$$G_{j}=\int_{F^{*}}
ho\left( \vec{V},\vec{n}
ight) dF,$$

where  $F^*$  is the throat surface,  $dF = 2\pi r dr$  is the surface element;  $\vec{n}$  stands for the normal vector to the integration surface.

# 4.1 Schlieren image and pressure field

In figure 3a) Schlieren image is presented, that has been obtained for model 1 in experiments in shock wind tunnel UT–1M facility, TsAGI, for  $p_{j,0} = 8$  bar. Detailed information on experimental setup and conditions of experiments is described in [18].

Figure 3b) illustrates calculated pressure field from numerical modeling of the above experiment. A shock arises from the nose of the sharp cone in supersonic flow and propagates downstream. Also are visible some shocks coming from the slot leading and trailing edges. It is

	$p_{j,0} = 1 \text{ bar}$	$p_{j,0} = 2 \text{ bar}$	$p_{j,0} = 4 \text{ bar}$	$p_{j,0} = 8 \text{ bar}$
model 1, 2	2.42	4.88	9.88	19.79
model 3	1.99	4.05	8.21	16.54

Table 1 Mass Flow Rate

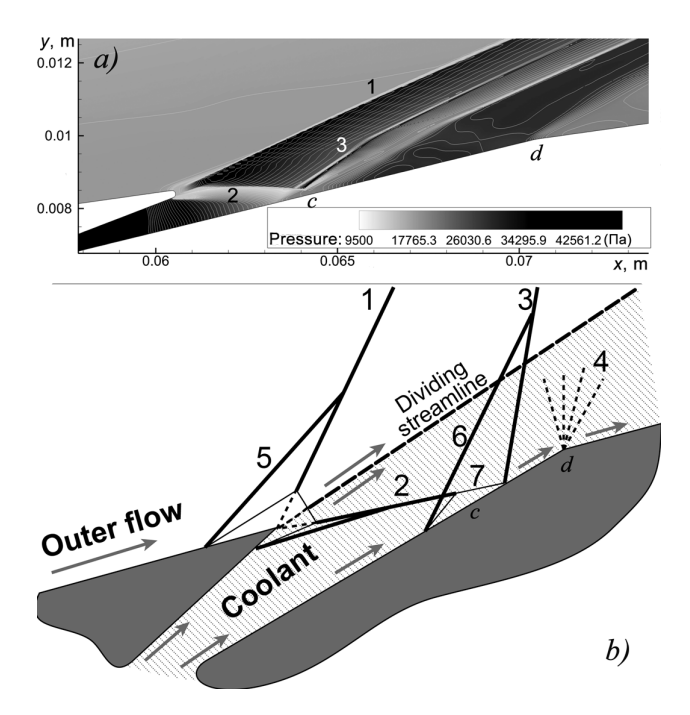


**Fig. 4** a) Calculated pressure field,  $p_{j,0} = 8$  bar; b) slot flow scheme. 1 — shock in outer flow; 2 — shock in coolant; 3 — 'reflected' shock; 4 — rarefaction fan; 5, 6 — shocks due to separations; 7 — separation bubble; c, d — reference points.

to be noted that injection leads to formation of some complicated flow structure which is a consequence of coolant/outer flow interaction.

#### 4.2 Slot Flow Scheme

It was not possible so far to distinguish all the features of flows interaction in details. Thus, let us consider the detailed flow pattern in the slot vicinity (see fig. 4).

Interaction of two streams of viscous gas at different pressures and velocities results in forming a complicated flow pattern. On the slot leading edge a dividing line emerges and mixing layer begins developing. Both outer flow and cooling gas need to change their direction to flow side by side. It is here when shock 1 in outer flow and shock 2 in coolant gas arise. The later falls onto

the slot trailing edge to form a separation bubble that in turn gives rise to a shock 3 of reattachment. Further the shocks 1 and 3 are combined to form a single shock in outer flow, which one may observe in fig. 3.

#### 4.3 Validation and Verification with Model 1

Fig. 5 illustrates a Stanton number St comparison of numerical results presented with various theoretical and experimental data:

$$St = \frac{q_w}{c_p \rho_\infty V_\infty (T_0 - T_w)},$$

where  $c_p$  stands for air heat capacity at constant pressure, while  $q_w$  is dimensional heat flux to the wall,  $\rho$  — density, V — velocity magnitude.

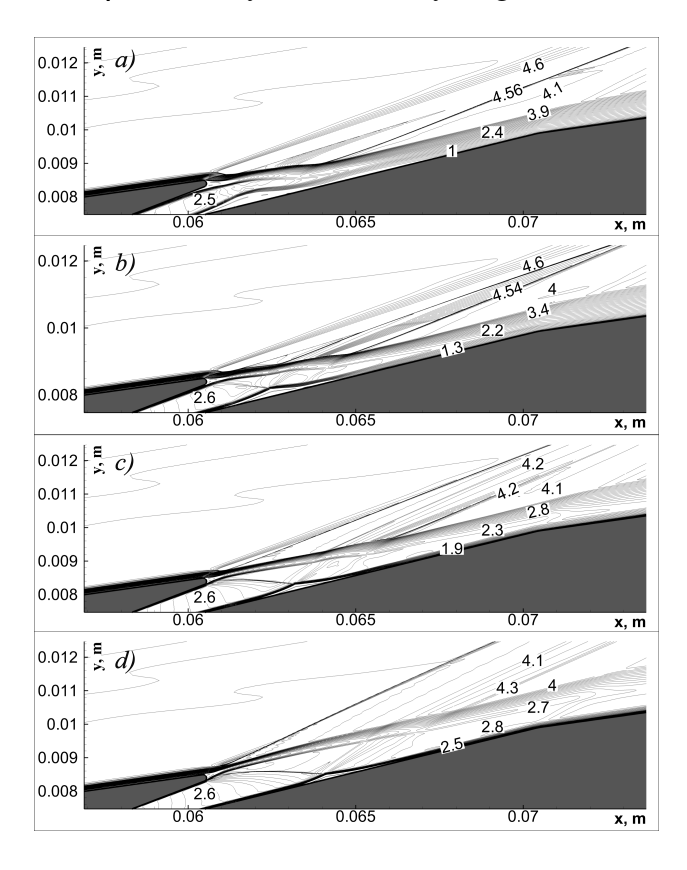


**Fig. 6** M isolines, model 1,  $p_{j,0}$  varies: a)—d) corresponds to 1, 2, 4, 8 bars, respectively

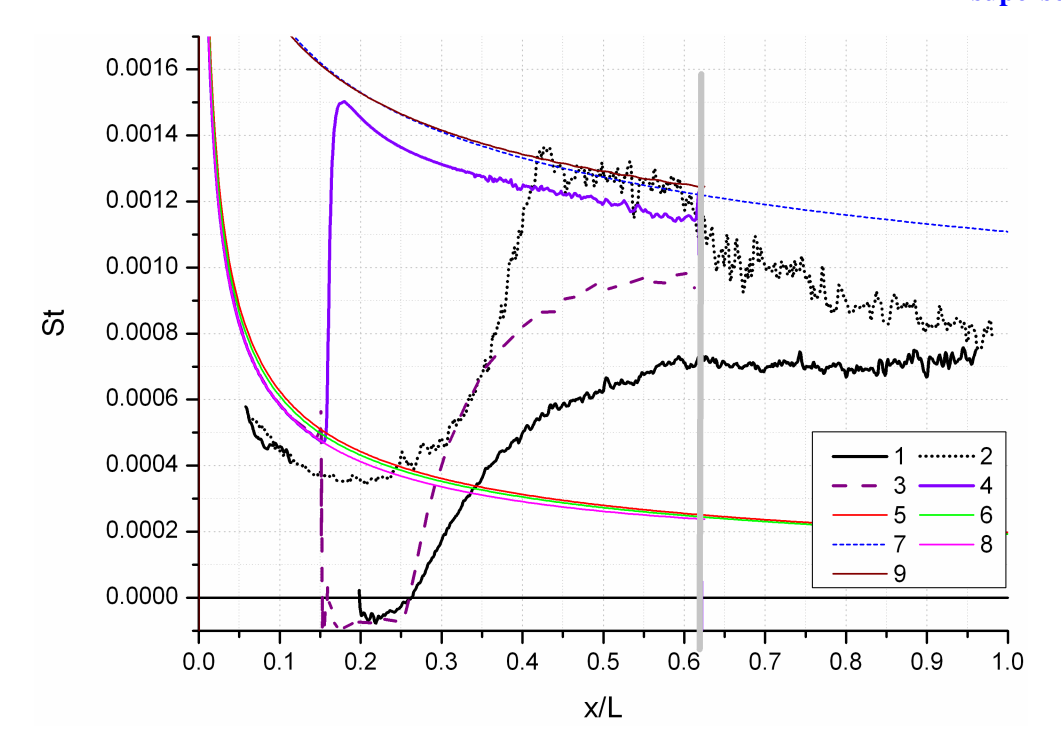


**Fig. 5** Results validation, St. 1 — experiment [18],  $p_{j,0} = 8$  bar; 2 — experiment [18], solid cone (no slot); 3 — Fluent,  $k - \omega$  transition SST,  $p_{j,0} = 8$  bar; 4 — Fluent, solid cone with forced LTT at slot leading edge; 5 — self-similar solution for laminar boundary layer over a sharp cone [19]; 6, 7 — experimental correlations for laminar and turbulent boundary layer, respectively [20]; 8, 9 — inhouse CFD code HSFlow TsAGI [21], laminar and turbulent calculations, respectively.

St number is presented versus dimensionless distance x/L along cone forming line where L is the length of experimental model 1 (400 mm). That of the model 1 has been taken 250 mm in calculations for the sake of numerical simplicity. As seen from fig. 5, LTT on solid cone without slot device takes place at the position of the slot (models 1, 3). This result can be relied on to confirm that the flow downstream the slot is fully turbulent. St curves 1 and 2 from experiment [18] shows the presence of cooling effect due to coolant injection. This effect is demonstrated using the numerical results in fig. 7 at different coolant mass rates which corresponds to  $p_{j,0} = 1, 2, 4, 8$  bar.  $St_s$  stands for calculated St on the solid cone. Laminar and turbulent branches of St calculated with Fluent are proved by other experimental correlations, known self-similar solutions and results of calculations with inhouse CFD code HSFlow TsAGI [21]. Numerical and experimental data are considered to be in satisfactory quantitative agreement. They are well

correlated in qualitative sense.

It is of interest that there is a region near the slot where heat flux becomes negative. This occurs because of two reasons. Firstly,  $T_{j,0} = T_w$  and Prandtl number Pr = 0.73 < 1. This leads to the fact that coolant recovery temperature is less than the wall one. Secondly, the boundary of mixing layer reaches the wall some distance apart the slot trailing edge. That is why there is a region next to the slot where the wall heats the coolant. Eventually, it should be noted that calculated and experimental lengths of this region coincide well. To verify numerical results, grid nodes (model 1) have been clustered twice stronger near the solid wall. That has not revealed any change in heat flux distribution calculated over model 1 surface.

### 4.4 Mach Number Fields

The paragraphs 4.4.1–4.4.3 contain figures 6–9 with following notations: a)–d) stand for total pressures of coolant  $p_{j,0} = 1,2,4,8$  bar, respectively.

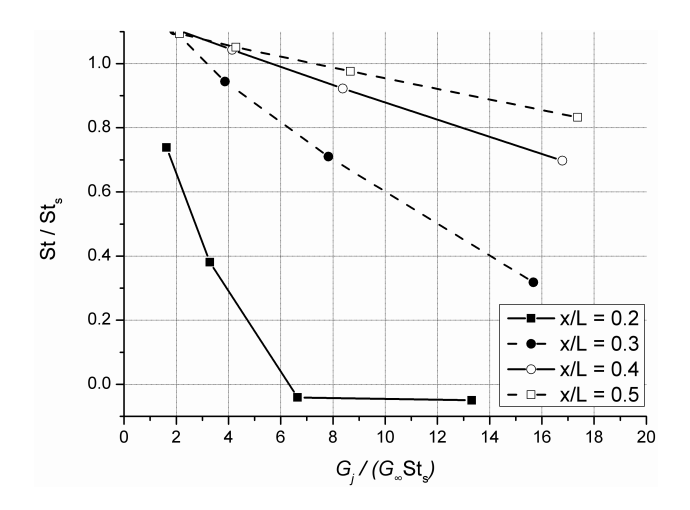


**Fig. 7** Computed cooling effect for various coolant mass rates at different locations

#### 4.4.1 Model 1

All separation regions are visible in the vicinity of the slot (see fig. 7). It is to be noted that coolant flows out the slot nozzle at supersonic speed. According to M distribution two flow schemes can be realized, namely: expansion and acceleration of outer flow downstream slot trailing edge; compression of outer flow in shock 1 (see fig. 4) formed at slot leading edge. In all cases shock 2 in coolant appears that leads to boundary layer separation at nozzle back wall and to formation of shock 3. The separation bubble 7 becomes shorter and moves downstream as  $p_{j,0}$  increases.

# 4.4.2 Model 2

For model 2 (see fig. 6) flow does not seem to separate coming to the porous piece of the surface at low  $p_{j,0}$ . Although it is not seen in fig. 6, there is a small separation zone before the slot. It is not closed, with coolant flowing there. Clustering Mach isolines denotes formation of a shock in outer flow that becomes more intense with the rise of coolant total pressure.

#### 4.4.3 Model 3

Flow structure becomes much more complicated in the case of injection through the model 3. Coolant coming out against outer flow effects in upstream direction causing the boundary layer to separate. Unfortunately, the coolant itself does

not appear to move in upstream direction. It tends to flow along the back nozzle wall and eventually reaches the cone surface. Increase of  $p_{j,0}$  results in displacing all recirculation regions to outer flow. Another separation bubble forms at the trailing edge. Coolant is forced to overcome this obstacle, which leads to change of outer flow direction. As a result, additional flow inhomogeneities arise, e.g. a shock on the cone surface that forms downstream the slot trailing edge.

# **4.5** Heat Fluxes Comparison for Models 1, 2, 3

In fig. 9, 10 dimensionless heat fluxes (St) are compared for all injection approaches under consideration at  $p_{j,0} = 4.8$  bar, when the cooling effect is more pronounceable. The notation is as follows: 0 stands for calculated results on solid cone, 1, 2, 3 — St over model 1, 2, 3.

It is clear that downstream injection (model 1) gives smooth behavior of St curves and turns out to produce the best cooling efficiency among all tested models. Nevertheless St curves are close to each other. This might imply that cooling efficiency slightly depends on the way the coolant is supplied.

# 4.6 Application: axisymmetric air inlet

Though St curves are close to each other, the flow structures for models 1, 2, 3 differs considerably. This note needs taking into account in applications. Let us consider a simple axisymmetric air inlet with conical central body. Suppose the inlet works at design conditions in the absence of slot device, i.e. the shock from the cone nose falls to a shell ring exactly (fig. 11).

Disturbances in the main stream due to the coolant injection result in change of mass rate and total pressure of gas in a section fixed on the cone surface — entrance section. It is possible to evaluate relative mass rate  $G_{rel}$  and average total pressure p0,rel across that section based on calculation results:

$$G_{rel} = \frac{G}{G_{\infty}} = \frac{\int_{R_1}^{R_2} \rho u \cdot 2\pi r dr}{\rho_{\infty} u_{\infty} \cdot F}$$

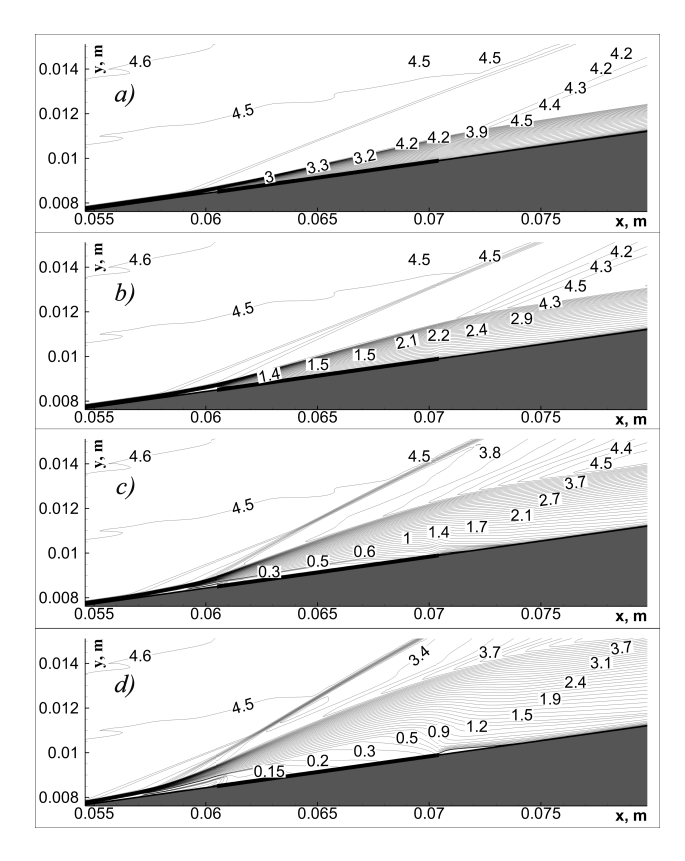


**Fig. 8** Mach number isolines, model 2,  $p_{j,0}$  varies: a) — d) corresponds to 1, 2, 4, 8 bars, respectively

$$p_{0,rel} = \frac{\bar{p}_0}{p_{0,\infty}} = \frac{\int_{R_1}^{R_2} p_0 \cdot 2\pi r dr}{p_{0,\infty} \cdot \pi \left(R_2^2 - R_1^2\right)}.$$

Here  $G_{\infty} = \rho_{\infty} V_{\infty} \pi R^2$ ,  $R = 35 \, mm$  is the magnitude of cone base radius.

Plots of  $G_{rel}$  and  $p_{0,rel}$  versus coolant total pressure  $p_{j,0}$  are shown in fig. 12 and 13, respectively. It is to be noted that the losses of total pressure and mass rate at the entrance of the imaginary inlet rise with the increase of  $p_{j,0}$ , which is due to intensifying the impact of the coolant on the outer flow. The losses of this kind would lead to drop in thrust. That is why it is of practical importance to find the optimum state between cooling efficiency and mechanical energy losses due to coolant / outer flow interaction.

In should be emphasized that injection in downstream direction shows the least impact on the outer flow compared with other considered ways of injection. Consequently, the resulting mechanical energy losses are the least. The biggest losses in total pressure are obtained for

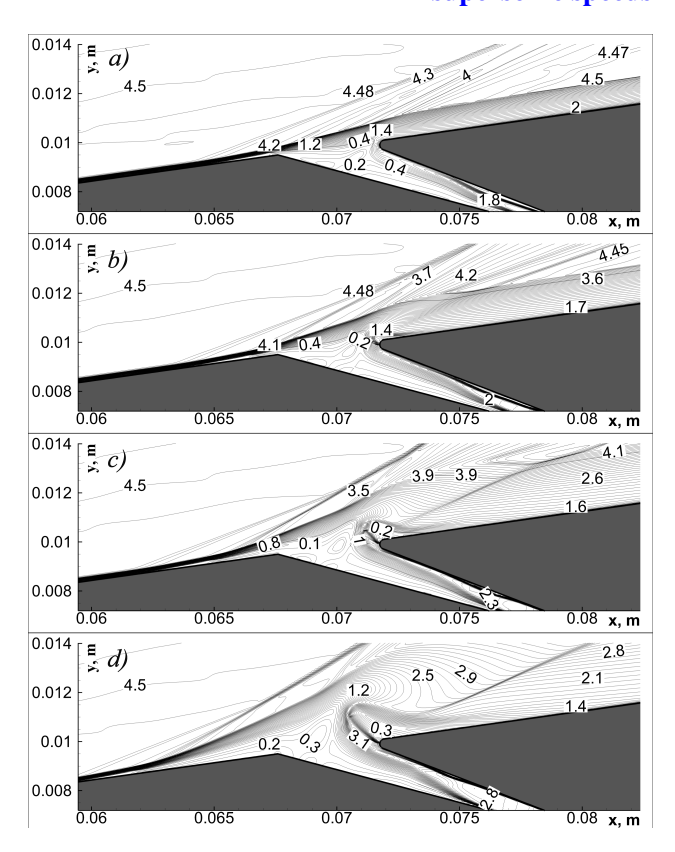


**Fig. 9** Mach number isolines, model 3,  $p_{j,0}$  varies: a)—d) corresponds to 1, 2, 4, 8 bars, respectively

model 3, with injection in upstream direction. Model 2 takes the intermediate position. Injection though the model 2 is found to produce nor better cooling efficiency nor less total pressure losses then that through the model 1.

#### 5 Conclusions

Film cooling of a sharp cone is investigated numerically. Three ways of coolant injection are considered. Flow structure in the slot vicinity is studied. Calculation results describe the general flow structure correctly from qualitative point of view, and in satisfactory quantitative agreement with various experimental data. Injection results in local effect of intensive cooling of the surface over a distance of several slot exit scales (from five to ten); cooling effectiveness decreases away from the slot. The most effective is injection in downstream direction. Analysis of total pressure losses is carried out for the case of simple axisymmetric air inlet with conical central body.

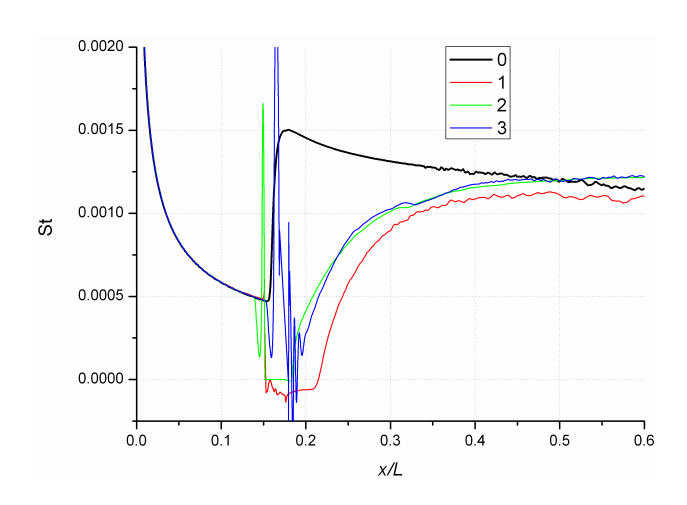


**Fig. 10** St distribution along cone generatrix,  $p_{i,0} = 4$  bar.

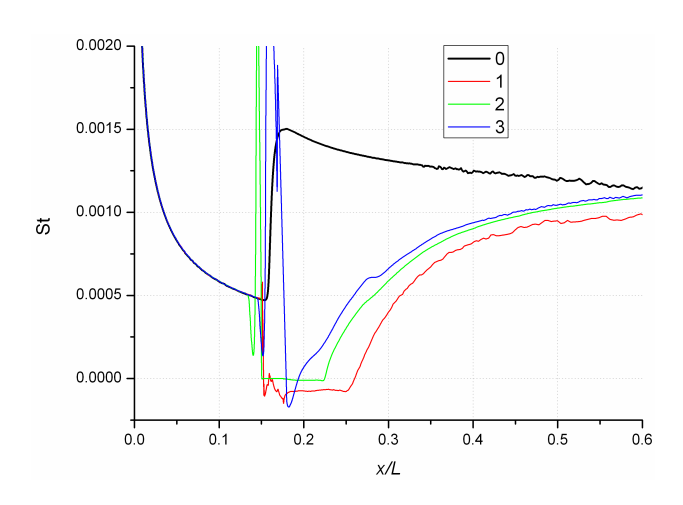


**Fig. 11** St distribution along cone generatrix,  $p_{i,0} = 8$  bar.

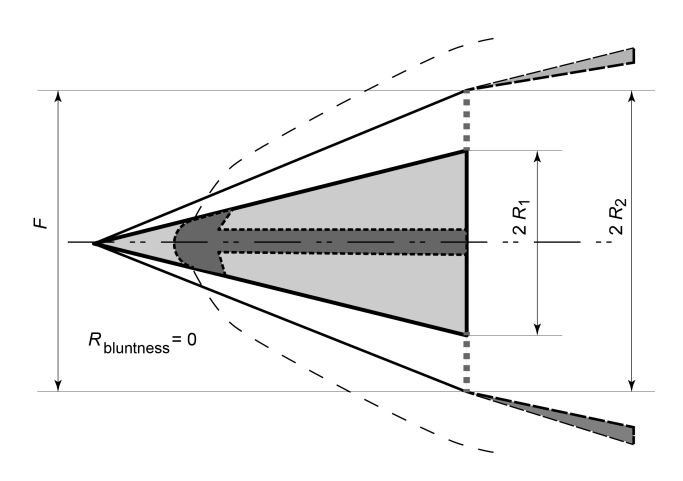


**Fig. 12** Axisymmetric air inlet scheme. Bold dotted gray line — inlet entrance

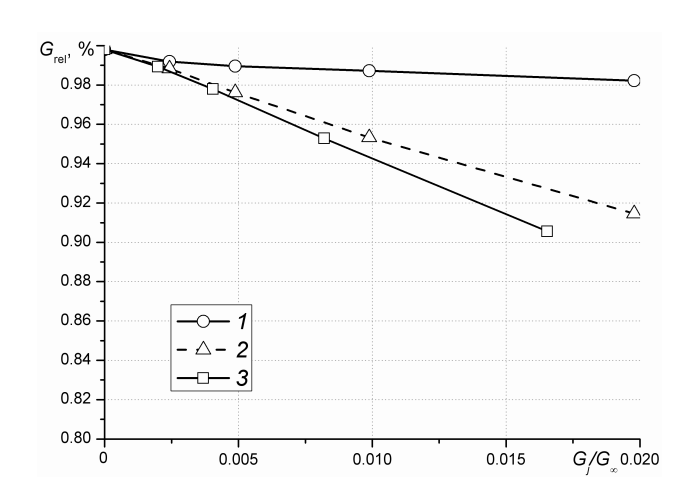


**Fig. 13**  $G_{rel}$  against  $G_j/G_{\infty}$ 

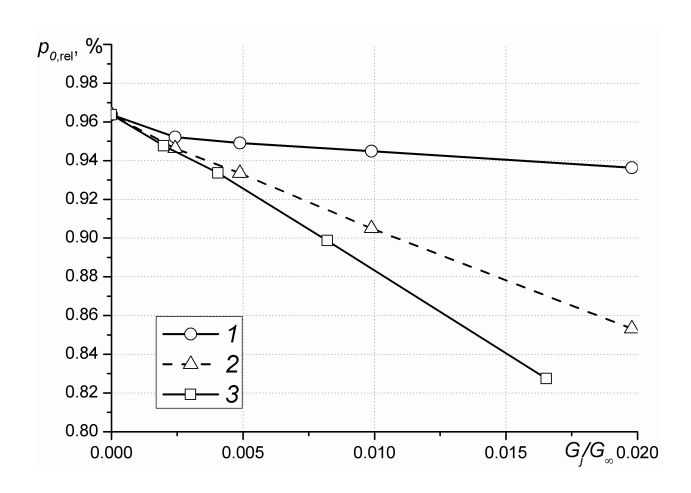


**Fig. 14**  $p_{0,rel}$  against  $G_j/G_{\infty}$ 

An increase in coolant total pressure and consequently in its mass rate leads to rise in mechanical energy losses. Injection in downstream direction leads to the least values of total pressure losses. Therefore, it is important to find an optimal state between cooling efficiency and the acceptable losses to implement film cooling protection systems on real configurations.

The work has been carried out in Moscow Institute of Physics and Technology (MIPT) with the financial support of Russian Scientific Foundation (project No. 14-19-00821).

#### **6 Contact Author e-mail Address**

pchdafe@gmail.com

# **Copyright Statement**

The authors confirm that they, and/or their company or organization, hold copyright on all of the original material included in this paper. The authors also confirm that they have obtained permission, from the copyright holder of any third party material included in this paper, to publish it as part of their paper. The authors confirm that they give permission, or have obtained permission from the copyright holder of this paper, for the publication and distribution of this paper as part of the ICAS 2014 proceedings or as individual off-prints from the proceedings.

#### References

- [1] C. Liess. Film cooling with injection from a row of inclined circular holes an experimental study for the application to gas turbine blades. In *Von Karman Institute for Fluid Dynamics, Technical note* 97, 1973.
- [2] D.E. Metzger, R.T. Baltzer, D.I. Takeuchi, and P.A. Kuenstler. Heat transfer to film-cooled combustion chamber liners. In ASME Paper No. 72-WA/HT-32, 1972.
- [3] J.J. Williams and W.H. Geidt. The effect of gaseous film cooling on the recovery temperature distribution in rocket nozzles. In *ASME Paper No. 70-HT/SpT-42*, 1970.
- [4] A.M. Jr. Cary and J.M. Hefner. Film cooling effectiveness in hypersonic turbulent flow. *AIAA Journal*, 8(11):2090–2091, 1970.
- [5] K. Parthasarathy and V. Zakkay. An experimental investigation of turbulent slot injection at Mach 6. *AIAA Journal*, 8(7):1302–1307, 1970.
- [6] J.N. Hefner, A.M. Jr. Cary, and D.M. Bushnell. Investigation of the three-dimensional turbulent flow downstream of swept slot injection in hypersonic flow. AIAA Paper, (74-679), 1974.
- [7] V. Zakkay and C.R. Wang. Investigation of multiple slot film cooling to a blunt nose cone. *AIAA Paper*, (73-698), 1973.
- [8] A.J. Srokowski, F.G. Howard, and M.V. Feller. Direct measurements at Mach 6 of turbulent skin friction reduction by injection from single and multiple flush slots. *AIAA Paper*, (76-178), 1976.

- [9] V.Ya. Borovoy, Ed.B. Vasilevsky, I.V. Struminskaya, and L.V. Yakovleva. Gas flow and heat protection by strong injection in the shock wave interference region near the blunt body front surface. In 3rd European symposium on Aerothermodynamics for space vehicles, ESA SP-426 Proceedings, 1998.
- [10] J. Linn and M.J. Kloker. Numerical investigations of film cooling and its influence on the hypersonic boundary-layer flow. Springer, RESPACE Key Technologies for Reusable Space Systems, NNFM, 98:151–169, 2008.
- [11] J. Linn, M. Keller, and M.J. Kloker. Effects of inclined blowing on effusion cooling in a Mach-2.67 boundary layer. In *Sonderforschungsbereich/Transregio* 40 — *Annual Report*, pages 55–67, 2010.
- [12] J. Linn and M.J. Kloker. Effects of wall-temperature conditions on effusion cooling in a Mach-2.67 boundary layer. *AIAA Journal*, 49(2):299–307, 2011.
- [13] M. Keller and M.J. Kloker. Numerical simulation of laminar film cooling in a supersonic boundary layer using modeled and simulated blowing. In *Sonderforschungsbereich/Transregio 40 Annual Report*, pages 43–57, 2011.
- [14] M. Keller and M.J. Kloker. Influence of boundary-layer turbulence on effusion cooling at Mach 2.67. In *Sonderforschungsbereich/Transregio* 40 *Annual Report*, pages 1–13, 2012.
- [15] K.A. Heufer and H. Olivier. Experimental and numerical study of cooling gas injection in laminar supersonic flow. *AIAA Journal*, 46(11):2741–2751, 2008.
- [16] M. Hombsch and H. Olivier. Flow condition and cooling gas variation for film cooling studies in hypersonic flow. In *Sonderforschungsbereich/Transregio 40 Annual Report*, pages 27–39, 2010.
- [17] M. Hombsch and H. Olivier. Film cooling in turbulent supersonic flow. In *Sonderforschungsbereich/Transregio 40 — Annual Report*, pages 19–29, 2011.

- [18] V.Ya. Borovoy, E.B. Vasilevskiy, I.V. Egorov, V.E. Mosharov, V.N. Radchenko, P.V. Chuvakhov, and V.V. Shtapov. Heat flux control by means of tangential air injection at high supersonic speeds. In 5th European Conference for Aeronautics and Space Sciences (EUCASS 2013), page on CD, 2013.
- [19] V.A. Bashkin. Raschet koeffitsientov soprotivleniya trenia i teploperedachi plastiny, konusa i tuponosogo tela v okrestnosti kriticheskoy tochki pri laminarnom techenii v pogranichnom sloe bez ucheta dissotsiatsii. *Trudy TsAGI, Materialy k raschetu soprotivleniya treniya i teploperedachi razlichnykh tel pri giperzvukovykh skorostyakh (in Russian)*, 937:13–21, 1964.
- [20] Avduevskiy V.S. and V.K. Koshkin. *Osnovy teploperedachi v aviatsionnoy i raketno-kosmicheskoy tekhnike*. M.:Mashinostroenie (in Russian), 1992.
- [21] I.V. Egorov, A.V. Federov, and V.G. Soudakov. Direct numerical simulation of disturbances generated by periodic suction-blowing in a hypersonic boundary layer. *Theor. Comput. Fluid Dyn.*, 20(1):41–54, 2006.